Two-Equation Diameter-PDF Transport Modeling of an evaporating poly-dispersed Droplet-laden Flow

R. Groll*, S. Jakirlić and C. Tropea

Fachgebiet Strömungslehre und Aerodynamik, Darmstadt University of Technology,
Petersenstrasse 30, 64287 Darmstadt, Germany

Keywords: Gas/liquid flow, a-α model, Euler/Euler approaches, four-eqn. turbulence model, liquid evaporation

ABSTRACT
This work addresses the modelling of evaporation in a droplet-laden gas flow within an Euler/Euler computational framework. Conventional modelling is generally based on the evaporation of single droplets, for instance using the model of Abramzon and Sirignano (1989). In the present study this modelling has been extended by introducing an additional transport equation for a newly defined quantity, a, known as the phase-interface surface fraction. This allows the drop diameter to be quantified in terms of a probability density function. The source term in the equation describing the dynamics of the volumetric fraction of the dispersed phase α^D is related to the evaporation time scale τ_Γ. The performance of the new model is evaluated using simulations of a poly-dispersed spray in a 3-D duct configuration.

1 Introduction

When simulating the motion of liquid drops in a dry gas it is important to capture not only the evaporation but also the interaction between the discrete and continuous phases. For instance strong evaporation rates influence the shear stress dynamics at the interface and the overall droplet drag in the air flow. Typical applications include fuel injection systems, spray drying in the foodstuff or pharmaceutical industries, or spray painting. Indeed, correct treatment of all transport phenomena (break-up, evaporation, combustion, etc.) is a pre-requisite for optimization of such multiphase systems.

Generally the kinematics of such multiphase systems is described using either an Euler/Euler or Euler/Lagrange scheme. In both approaches the continuous phase is simulated using a field (Euler) description. While the Euler/Euler approach also simulates the disperse phase using a field description, the Euler/Lagrange approach uses a material description of the disperse phase, computing individual particle trajectories.

Accounting for the interaction between discrete and continuous phase followed by a phase interchange due to disperse phase evaporation is of decisive importance when simulating the motion of liquid drops in a dry gas. The evaporation rate at the interfacial surface and the relative humidity influences strongly the shear stress dynamics and the drag rates of continuous phase. The direct injection of a Diesel spray (break-up, evaporation and combustion are occurring sequentially) or spray drying in food or chemical industry are only two illustrative examples for industrial research areas, which uses powerful optimization tools for the prediction of multiphase transport processes. The capability of a computational scheme to account for all important phenomena featuring these processes is a major prerequisite for successful optimization of many industrial, multiphase systems. Most widely used computational schemes describing the kinematics of such multiphase processes are the Euler/Euler and the Euler/Lagrange approachs. The velocity and other physical values of the continuous carrier phase are simulated by the spacial Eulerian description in both approaches. While the particle velocity is simulated as well in the Euler/Euler approach the Euler/Lagrangian description is simulation the ways of the dispersed drops, called particle trajectories. For both approaches the interaction of droplet and carrier phase is given by mass, momentum and heat exchange, which has to be modeled additionally. Although the numerical stability and robustness shows the high advantage of the Euler/Lagrange approach, its disadvantage, the high numerical load, is noteworthy as well. The alternative approach, the Euler/Euler approach, which describes the two phase flow as two interpenetrating continua, which are defined by a set set of spacial equations which governs both phases. The volume fractions of the continuous α^C and the dispersed phase α^D are given by new variables. The sum of the volume fraction of all participating phases is equal one. Turbulence describing values of the dispersed particle phase are most often modeled by one equation for the transport of the turbulent kinetic energy or an algebraic modeled turbulent viscosity. The model of the present work is in line with the model proposed by *He and Simonin* [4] and differs from standard models with the covariance transport. This value integrates the correlation of the particle and the carrier phase velocities.

2 Computational Method

A large number of statistical turbulence models for single-phase flows defining the Reynolds-stress tensor, whose gradient originate from the (convective) turbulent transport of momentum, have been developed in the past. The most widely used are those based on the Boussinesq's analogy employing eddy viscosity as a model parameter. This model group 'transforms' the Reynolds-stress gradient into a diffusion-like transport term. Such a diffusion term does not result from the interaction between turbulent eddies in the two-phase flows; here, turbulent transport has a somewhat different nature due to non-viscous character of the particles.

The turbulent motion of the particles is represented by mixing of particle clouds. In this work, a four-equation model is used to mimic the transport of turbulence in both dispersed and continuous phase. The transport of the kinetic energy of turbulence of both phases, the dissipation rate of the continuous phase and the covariance of the velocities of both phases

---

*Corresponding author: groll@sla.tu-darmstadt.de

are defined with these four equations. The complete specification of the background model could be found elsewhere (see e.g., Groll et al., 2003) [3], here only details related to the evaporation modelling will be given.

2.1 Evaporation dependent Diameter PDF

In an evaporating process, the mass transfer rate on the drop surface depends on the drop size. The polydispersed spray consists of drops with different diameters. To determine the mass transfer, i.e. the evaporation rate for such a case, the drop diameter distribution of the spray is necessary. Using the approach based on a *particle diameter probability density function* (PDF), Groll (2002) (see Fig. 1a for its graphical representation):

$$f\left(\frac{D_p}{\mathsf{E}\left(D_p\right)}\right) \quad = \quad \frac{\pi}{2}\frac{D_p}{\mathsf{E}\left(D_p\right)}e^{-\frac{\pi}{4}\frac{D_p^2}{\mathsf{E}(D_p)^2}} \tag{1}$$

$$\text{where } f\left(D_p\right) \quad = \quad \frac{9}{8}\pi\frac{D_p}{D_{32}^2}e^{-\frac{9}{16}\pi\frac{D_p^2}{D_{32}^2}} \quad \text{with } D_{32} = \frac{\mathsf{E}\left(D_p^3\right)}{\mathsf{E}\left(D_p^2\right)} = \frac{6\bar{\alpha}^D}{\bar{a}} \tag{2}$$

depending on the Sauter mean diameter the mass transfer rate can be calculated. The expectation values of the squared and cubic diameters in terms of the Sauter mean diameter only, result from this modelled PDF:

$$\mathsf{E}\left(D_p\right) = \frac{2}{3}D_{32} \qquad \mathsf{E}\left(D_p^2\right) = \frac{16}{9\pi}D_{32}^2 \qquad \mathsf{E}\left(D_p^3\right) = \frac{16}{9\pi}D_{32}^3 \tag{3}$$

A time dependent relation has to be defined to calculate the change of the drop diameter when simulating motion of a
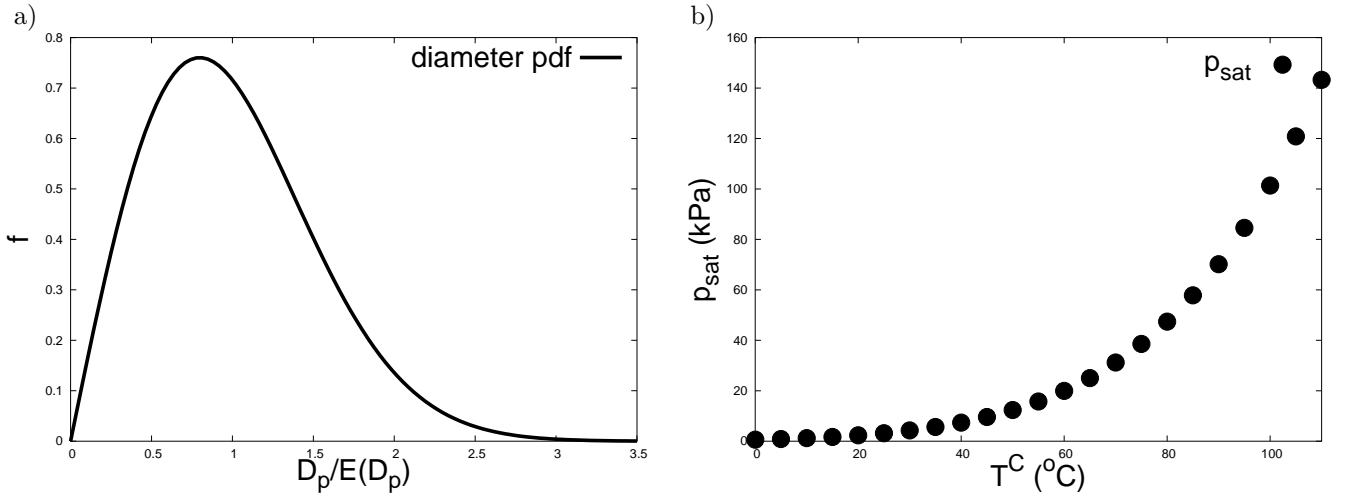
a)

b)

Figure 1: a) PDF of a normalized particle drop diameter in a polydisperse spray and b) temperature dependent saturation pressure curve

polydispersed phase. The change of the expectation value of the diameter squared is presumed to be constant in accordance to the d^2-law, Kastner (2001):

$$\frac{\mathsf{d}}{\mathsf{d}t}\mathsf{E}\left(D_p^2\right) = -\Gamma \quad . \tag{4}$$

Integration of this equation results in the time-dependent solution for the drop diameter:

$$D_p(t) = \sqrt{D_p^2(0) - \Gamma t} \quad . \tag{5}$$

Substitution of the expectation value with the given density function definition

$$-\Gamma = \frac{\mathsf{d}}{\mathsf{d}t}\mathsf{E}\left(D_p^2\right) = \frac{16}{9\pi}\frac{\mathsf{d}}{\mathsf{d}t}D_{32}^2 \;\Rightarrow\; -\frac{9\pi}{16}\Gamma = \frac{\mathsf{d}}{\mathsf{d}t}D_{32}^2 = 2D_{32}\frac{\mathsf{d}}{\mathsf{d}t}D_{32} \;\Rightarrow\; \dot{D}_{32} = -\frac{9\pi}{32}\frac{\Gamma}{D_{32}} \tag{6}$$

reveals that the deviation of the Sauter mean diameter depends on the evaporation constant of the d^2-law. Based on this formulation, the following equation has been derived:

$$\frac{\mathsf{d}}{\mathsf{d}t}\mathsf{E}\left(D_p^3\right) \quad = \quad \frac{16}{9\pi}\frac{\mathsf{d}}{\mathsf{d}t}D_{32}^3 = \frac{16}{9\pi}\left(\dot{D}_{32}D_{32}^2 + D_{32}\frac{\mathsf{d}}{\mathsf{d}t}D_{32}^2\right) = \frac{16}{9\pi}\left(-\frac{9\pi}{32}\frac{\Gamma}{D_{32}}D_{32}^2 - \frac{9\pi}{16}\Gamma D_{32}\right)$$

$$= \quad -\Gamma D_{32} - \frac{1}{2}\Gamma D_{32} = -\frac{3}{2}\Gamma D_{32} \quad . \tag{7}$$

With this expression, the time-dependent change of an expected drop volume is defined. The outcome of the last equation is used for the determination of the mass transfer of a drop with the expected mass $\bar{m}_p$:

$$\frac{\mathsf{d}\bar{m}_p}{\mathsf{d}t} = \frac{\pi}{6}\rho^D\frac{\mathsf{d}}{\mathsf{d}t}\mathsf{E}\left(D_p^3\right) = -\frac{\pi}{4}\rho^D D_{32}\Gamma \quad . \tag{8}$$

Based on the evaporation model due to *Abramzon and Sirignano* [1], the mass transfer rate at the surface of a drop representing a function of the Sherwood number Sh and the mass transfer coefficient B_M

$$B_M \quad = \quad \frac{Y_{\text{sat}} - Y_\infty}{1 - Y_{\text{sat}}} = \frac{Y_{\text{sat}}}{1 - Y_{\text{sat}}} - \frac{Y_\infty}{1 - Y_{\text{sat}}} = \frac{0,622 p_{\text{sat}} - Y_\infty \left(p - 0,378 p_{\text{sat}}\right)}{p - p_{\text{sat}}} \quad , \tag{9}$$

both depending on the saturation pressure p_{sat} (see Fig. 1b) and the absolute humidity of the saturated gas phase Y_{sat}

$$\frac{Y_{\text{sat}}}{1 - Y_{\text{sat}}} = 0,622 \frac{p_{\text{sat}}}{1 - p_{\text{sat}}} \quad , \tag{10}$$

is to be determined by using the following equation:

$$\dot{m} = \pi D_{21} \rho^C D_{\alpha\beta} Sh B_M \quad . \tag{11}$$

The humidities Y_{sat} and Y_∞ are related to the limiting cases of a complete saturated gas phase and far away from a droplet. The definition of the Sherwood number Sh and its modification are given in the subchapter *heat transfer*. By equalizing the PDF-dependent mass transfer rate and the modelled mass transfer rate, the evaporation constant in the model of *Abramzon and Sirignano* is defined as:

$$\frac{\pi}{4} \rho^D D_{32} \Gamma \quad = \quad -\dot{m}_p = \dot{m} = \pi D_{21} \rho^C D_{\alpha\beta} Sh B_M \Rightarrow \Gamma = 4 \frac{D_{21}}{D_{32}} \frac{\rho^C}{\rho^D} D_{\alpha\beta} Sh B_M \quad . \tag{12}$$

In accordance to the d^2-law, the evaporation constant should be independent of the particle diameters. This fact brings an additional constraint to the expectation values of the probability function:

$$\frac{D_{21}}{D_{32}} = \text{const.} \tag{13}$$

The given PDF fulfills this condition as follows:

$$\frac{D_{21}}{D_{32}} = \frac{\mathsf{E}\left(D^2\right) \mathsf{E}\left(D^2\right)}{\mathsf{E}\left(D\right) \mathsf{E}\left(D^3\right)} = \frac{8}{3\pi} \quad . \tag{14}$$

With the proposal of *Abramzon and Sirignano*, the time-dependent modelling of the drop diameter probability function is closed.

2.2 Evaporation Progress

The model developed serves for calculation of the evaporation rate of spherical water drops. Water is a liquid dispersed phase, which satisfies the d^2-law. Keeping in mind the definition of the life time of a drop T and its diameter loss rate (Eq. 5), it is known, that each drop with a diameter

$$D_p < \sqrt{\Gamma T} \tag{15}$$

is to evaporate completely. To determine the number of the evaporated drops in a cloud, the probability density function has to be integrated in the following way:

$$\int_0^{\sqrt{\Gamma T}} f\left(D_p\right) \, \mathrm{d}D_p \quad . \tag{16}$$

Consequently, the time change of the particle number is obtained as follows:

$$\frac{\mathrm{d}}{\mathrm{d}t} \bar{n} \quad = \quad -\lim_{T \to 0} \left[\frac{\bar{n}}{T} \int_0^{\sqrt{\Gamma T}} f\left(D_p\right) \, \mathrm{d}D_p \right] = \lim_{T \to 0} \left[\frac{\bar{n}}{T} \left(e^{-\frac{9\pi}{16} \frac{\Gamma T}{D_{32}^2}} - 1\right)\right]$$

$$= \quad \lim_{T \to 0} \left[\frac{\bar{n}}{T} \left(e^{mT} - 1\right)\right] \qquad \left(\text{where } m = -\frac{9\pi}{16} \frac{\Gamma}{D_{32}^2}\right) \tag{17}$$

$$= \quad \lim_{T \to 0} \left[\frac{\bar{n}}{T} \left((1 + mT)^{\frac{1}{mT} \cdot mT} - 1\right)\right] = \lim_{T \to 0} \left[\frac{\bar{n}}{T} \cdot mT\right] = \bar{n} \cdot m = -\frac{9\pi}{16} \frac{\Gamma}{D_{32}^2} \bar{n} \quad . \tag{18}$$

The time change of the volumetric fraction

$$\bar{\alpha}^D = \bar{n} \cdot \frac{\pi}{6} \mathsf{E}\left(D_p^3\right) \tag{19}$$

is calculated by using the results represented by Eqs. (7) and (18).

$$\frac{\mathrm{d}}{\mathrm{d}t} \bar{\alpha}^D \quad = \quad \frac{\pi}{6} \mathsf{E}\left(D_p^3\right) \frac{\mathrm{d}}{\mathrm{d}t} \bar{n} + \bar{n} \frac{\pi}{6} \frac{\mathrm{d}}{\mathrm{d}t} \mathsf{E}\left(D_p^3\right) \quad = -\frac{\pi}{6} \frac{16}{9\pi} D_{32}^3 \cdot \frac{9\pi}{16} \frac{\Gamma}{D_{32}^2} \bar{n} - \bar{n} \frac{\pi}{6} \cdot \frac{3}{2} \Gamma D_{32}$$

$$= \quad -\bar{n} \frac{\pi}{6} \Gamma D_{32} \left(1 + \frac{3}{2}\right) = -\frac{45}{32} \pi \frac{\Gamma \bar{\alpha}^D}{D_{32}^2} \tag{20}$$

The time change of the Sauter mean diameter consists of the deviations of the volumetric fraction and the surface fraction:

$$D_{32} = 6\frac{\bar{\alpha}^D}{\bar{a}} \Rightarrow \dot{D}_{32} = \frac{6}{\bar{a}^2}\left(\bar{a}\frac{\mathrm{d}}{\mathrm{d}t}\bar{\alpha}^D - \bar{\alpha}^D\frac{\mathrm{d}}{\mathrm{d}t}\bar{a}\right) = \underbrace{6\frac{\bar{\alpha}}{\bar{a}}}_{D_{32}}\left(\frac{1}{\bar{\alpha}^D}\frac{\mathrm{d}}{\mathrm{d}t}\bar{\alpha}^D - \frac{1}{\bar{a}}\frac{\mathrm{d}}{\mathrm{d}t}\bar{a}\right) \tag{21}$$

Utilizing the results following from the Eqs. (6) and (20), the change of the surface fraction can also be formulated in terms of the evaporation constant and the Sauter mean diameter:

$$\frac{1}{\bar{a}}\frac{\mathrm{d}}{\mathrm{d}t}\bar{a} = \frac{1}{\bar{\alpha}^D}\frac{\mathrm{d}}{\mathrm{d}t}\bar{\alpha}^D - \frac{1}{D_{32}}\frac{\mathrm{d}}{\mathrm{d}t}D_{32} = -\frac{45\pi}{32}\frac{\Gamma}{D_{32}^2} + \frac{9\pi}{32}\frac{\Gamma}{D_{32}^2}$$

$$= -\frac{9\pi}{8}\frac{\Gamma}{D_{32}^2} \quad\Rightarrow\quad \frac{\mathrm{d}}{\mathrm{d}t}\bar{a} = -\frac{9\pi}{8}\frac{\Gamma}{D_{32}^2}\bar{a} \quad . \tag{22}$$

The source terms of the α-equation (Eq. 20) and the a-equation (Eq. 22) stay in following relationship:

$$\frac{1}{\bar{\alpha}^D}\frac{\mathrm{d}}{\mathrm{d}t}\bar{\alpha}^D = \frac{5}{4}\cdot\frac{1}{\bar{a}}\frac{\mathrm{d}}{\mathrm{d}t}\bar{a} \quad . \tag{23}$$

Obviously, the source terms in both transport equations can be formulated in terms of the same parameter: τ_Γ (Eq. 26). With the definition of the particle diameter probability density function as the starting point, the evaporation process is finally modelled by the following two transport equations:

$$\partial_t\left(\rho^D\bar{\alpha}^D\right) + \partial_j\left(\rho^D\bar{\alpha}^D <u_j^D>^D\right) = -\frac{5}{4}\rho^D\tau_\Gamma^{-1}\bar{\alpha}^D \tag{24}$$

$$\partial_t\left(\rho^D\bar{a}\right) + \partial_j\left(\rho^D\bar{a} <u_j^D>^D\right) = -\rho^D\tau_\Gamma^{-1}\bar{a} \tag{25}$$

The convective transport in both equations is defined by the volume-fraction-weighted averaged particle velocity $<u_i^D>^D$ [8]. The first equation (Eq. 24) originates from the well-known mass balance of the dispersed phase with a mass transfer defining source term. The second equation (Eq. 25) governs the surface fraction of the dispersed phase, being the synonym for the cloud surface per volume. The evaporation time scale τ_Γ, the source terms of this evaporation-describing two-equation model depend upon, reads:

$$\tau_\Gamma = -\bar{a}\left(\frac{\mathrm{d}}{\mathrm{d}t}\bar{a}\right)^{-1} = \frac{8}{9\pi}\frac{D_{32}^2}{\Gamma} \quad . \tag{26}$$

Accordingly, the transport of both quantities α^D and a depends on the evaporation constant Γ, which is given by the d^2-law. Introducing the definition of the evaporation constant, the final expression serving for the determination of the evaporation time scale is given by:

$$\tau_\Gamma = \frac{D_{32}^2}{12}\frac{\rho^D}{\rho^C}\left(D_{\alpha\beta}\mathsf{Sh}B_M\right)^{-1} \quad . \tag{27}$$

By solving the equations of the α-a model, the evaporation rate of a spray stream can be quantified. In such a way, the mass balance of a two-phase flow is completely satisfied.

2.3 Heat transfer

Starting from the initial definitions of *Nusselt* and *Sherwood* Numbers

$$\mathsf{Nu}_0 = 1 + \left(1 + \mathsf{Re}_{\mathsf{rel}}\,\mathsf{Pr}\right)^{\frac{1}{3}}\cdot f\left(\mathsf{Re}_{\mathsf{rel}}\right) \quad , \quad \mathsf{Sh}_0 = 1 + \left(1 + \mathsf{Re}_{\mathsf{rel}}\,\mathsf{Sc}\right)^{\frac{1}{3}}\cdot f\left(\mathsf{Re}_{\mathsf{rel}}\right)$$

$$\text{with} \quad f\left(\mathsf{Re}_{\mathsf{rel}}\right) = \left|\begin{array}{ll} 1 & ;\ \mathsf{Re}_{\mathsf{rel}} \leq 1 \\ \mathsf{Re}_{\mathsf{rel}}^{0,077} & ;\ \text{else} \end{array}\right| \tag{28}$$

$$\text{and} \quad \mathsf{Re}_{\mathsf{rel}} = \frac{\rho^C\left|\vec{u}^D - \vec{u}^C\right|\mathsf{E}\left(D_p\right)}{\mu^C} \quad , \quad \mathsf{Pr} = \frac{c_p^C\mu^C}{\lambda^C} \quad , \quad \mathsf{Sc} = \frac{\mu^C}{\rho^C D_{\alpha\beta}} \tag{29}$$

the modifications due to *Abramzon and Sirignano* [1] are defined in the following way:

$$2 + \frac{\mathsf{Sh}_0 - 2}{F\left(B_M\right)} = \mathsf{Sh}^* = \mathsf{Sh}\frac{B_M}{\ln\left(1 + B_M\right)} \quad , \quad 2 + \frac{\mathsf{Nu}_0 - 2}{F\left(B_T\right)} = \mathsf{Nu}^* = \mathsf{Nu}\frac{B_T}{\ln\left(1 + B_T\right)} \tag{30}$$

$$\text{with} \quad F\left(B\right) = \left(1 + B\right)^{0,7}\frac{\ln\left(1 + B\right)}{B} \quad , \quad \mathsf{Le} = \frac{\mathsf{Sc}}{\mathsf{Pr}} = \frac{\lambda^C}{\rho^C c_p^C D_{\alpha\beta}} \quad . \tag{31}$$

Introducing these modified *Sherwood* and *Nusselt* numbers into the mass transfer equation

$$\dot{m} = \pi D_{21}\frac{\lambda^C}{c_p^D}\mathsf{Nu}^*\ln\left(1 + B_T\right) \quad , \quad \dot{m} = \pi D_{21}\rho^C D_{\alpha\beta}\mathsf{Sh}^*\ln\left(1 + B_M\right) \tag{32}$$

$$\Rightarrow \quad \frac{c_p^C}{c_p^D}\underbrace{\frac{\lambda^C}{\rho^C c_p^C D_{\alpha\beta}}}_{=\mathsf{Le}}\mathsf{Nu}^*\ln\left(1 + B_T\right) = \mathsf{Sh}^*\ln\left(1 + B_M\right) \tag{33}$$

4

the exponent ϕ_B featuring in the heat transfer coefficient (HTC) equation

$$B_T = (1 + B_M)^{\phi_B} - 1 \tag{34}$$

arises from Eq. (33):

$$\phi_B = \frac{\ln\left(1 + B_T\right)}{\ln\left(1 + B_M\right)} = \frac{c_p^D}{c_p^C}\frac{\mathsf{Sh}^*}{\mathsf{Nu}^*}\mathsf{Le}^{-1} \qquad . \tag{35}$$

The heat flux

$$Q_L = \mathsf{Nu}\pi D_{21}\lambda^C\left(T^C - T^D\right) - \dot{m}\,L\left(T^D\right) \tag{36}$$

depending on the *Nusselt* number Nu can also be described by B_T and the liquid temperature dependent latent heat $L(T^D)$:

$$B_T = \frac{c_p^D\left(T^C - T^D\right)}{Q_L/\dot{m} + L\left(T^D\right)} \qquad \Rightarrow \qquad Q_L = \dot{m}\left(\frac{c_p^D\left(T^C - T^D\right)}{B_T} - L\left(T^D\right)\right) \qquad . \tag{37}$$

Utilizing the heat flux definition given by Eq. (36), the mass transfer rate formulae can be finally written as a function of the *Nusselt number*:

$$\dot{m} = \pi D_{21}\frac{\lambda^C}{c_p^D}\mathsf{Nu}B_T \qquad . \tag{38}$$

In such a way, the mass transfer from the liquid to the gas phase can be determined. Here, the *Nusselt* number is calculated using the algorithm outlined below (note that the *Sherwood* number and the mass transfer coefficient are defined by Eq. (30) and (9) respectively). Starting from its initial value

$$\mathsf{Nu}^{*(0)} = \mathsf{Nu}_0 \qquad . \tag{39}$$

the following iterative algorithm is used for the *Nusselt* number determination:

$$\phi_B^{(n)} = \frac{c_p^D}{c_p^C}\frac{\mathsf{Sh}^*}{\mathsf{Nu}^{*(n)}}\mathsf{Le}^{-1}\,, \quad B_T^{(n+1)} = \left(1 + B_M\right)^{\phi_B^{(n)}} - 1\,, \quad \mathsf{Nu}^{*(n+1)} = 2 + \frac{\mathsf{Nu}_0 - 2}{F\left(B_T^{(n+1)}\right)} \qquad . \tag{40}$$

The truncation condition is defined by the ratio of the heat transfer coeficients : $\left|\frac{B_T^{(n+1)}}{B_T^{(n)}} - 1\right| < \epsilon$.

Herewith, the computational scheme describing the processes of the heat and mass transfer in an evaporating two-phase flow is completed. As a conclusion, one can say that additional source terms in the equations of the continuous phase show, that evaporation rate written in terms of the evaporation time scale τ_Γ exhibits similar effects on the turbulence as the drag forces, modelled in terms of the relaxation time scale τ_p [3]. Due to the evaporation of the dispersed phase, the influence of the mass transfer rate is restricted only on the volumetric fraction of the dispersed phase and has no influence on its turbulent kinetic energy.

RESULTS

The derived model is demonstrated using a water spray evaporating in a fully developed duct flow. As an illustration of the model performance, some selected results are shown in Figs. 2-3. In order to provide the fully-developed air flow and turbulence conditions, a completely saturated gas phase (relative humidity was taken to be 100%, large dark area in Fig. 2) was computed over the duct length of $260h = 5.2m$ (h-channel half-width), prior to the onset of the evaporation process. After this length the turbulent two-phase channel flow becomes fully developed. The initial value of the temperature taken in this region is $353K$. The water drops with a mean diameter of $100\mu m$ are introduced in the air flow. Downstream of this region the liquid phase evaporation is introduced by heating the duct walls up to the temperature of $368K$ (in such a way the temperature gradient corresponding to the difference between initial value prescribed at the inlet cross-section - $x = 0$ - and the constant wall temperature was imposed) causing a decrease in the relative humidity, Fig. 2. Consequently, the mean drop diameter decreases too, Fig. 3. Because of the saturation pressure gradient maximum (dY_{sat}/dT) near the boiling point at 373K (Fig.1b), the gas temperature is chosen to be between 353K and 368K. In order to prevent the boiling of the water drops, the wall temperature has to be lower than the boiling temperature.
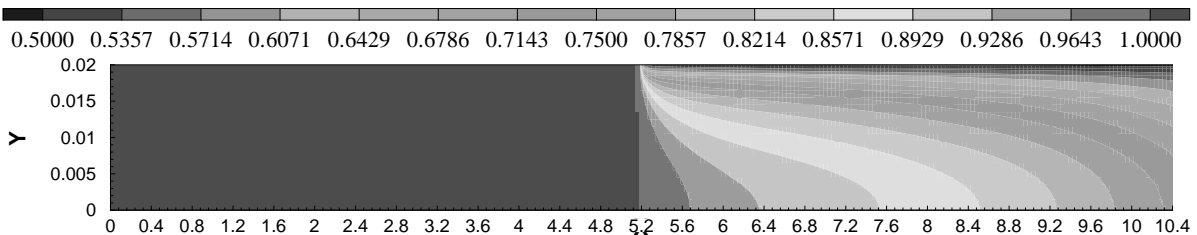

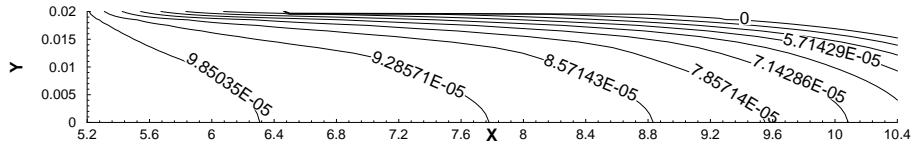Figure 2: Distribution of the relative humidity obtained by the present Euler/Euler scheme

Fig. 3: Droplet diameter isolines obtained by the present Euler/Euler scheme

Fig. 4a displays the evolution of the mass transfer coefficients B_M in the Abramzon and Sirignano evaporation model. This coefficient, representing indeed a measure of the vapor fraction being absorbed by the surrounding gas phase, increases due to warm up of the gas phase, because of the decreasing relative humidity. The ratio of the droplet surface to the droplet volume increases by the droplet diameter reduction (Fig. 3). Due to the temperature raise, resulting in the intensification of the evaporating process, the time scale of the evaporation is decreasing, Fig. 4b.
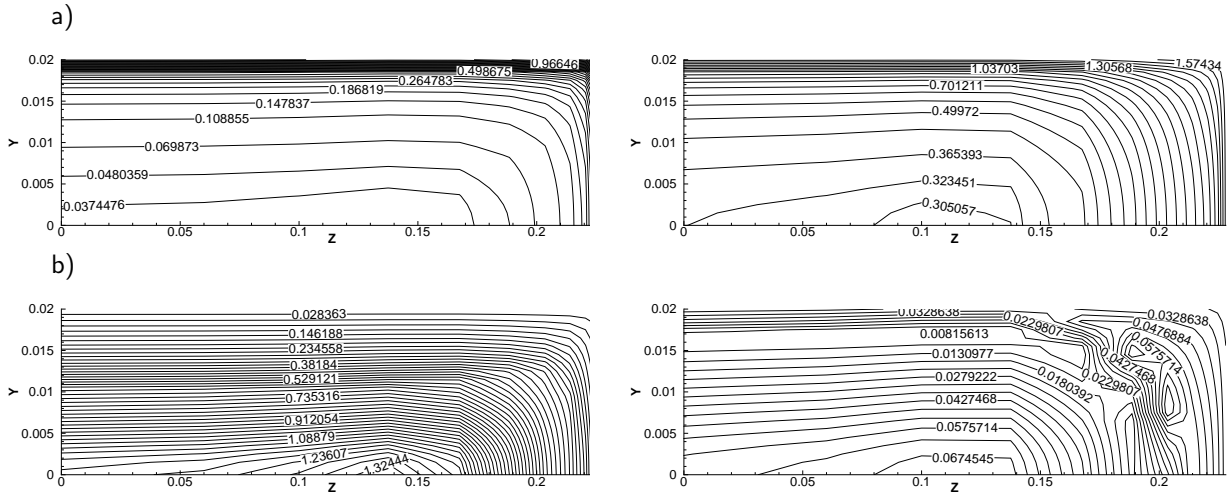
a)

b)

Figure 4: Isolines of a) mass transfer coefficients B_M and b) time scale of evaporation τ_Γ (in seconds) across the duct at two selected longitudinal locations $x/h = 20$ (left) and 140 (right) obtained by the present Euler/Euler scheme

CONCLUSIONS

Based on a new two-equation model the transport of the mean drop diameter in a dispersed two-phase flow has been developed using a coupling mechanism based on the predicted pdf. Using this model the mutual influence of the two phases on each other are quantified in terms of transport equations of $\overline{a}$ and $\overline{\alpha^D}$.

Based on the definition of an evaporation or mass transfer time scale τ_Γ the drop specific model of the local mass transfer rate near a single drop can be extrapolated to a global mass transfer rate considering the distribution of drop sizes. During the change of the mean drop size the influence on interaction of momentum and turbulence is also quantified applying this model.

References

[1] B. Abramzon und W. A. Sirignano : Droplet Vaporization Model for Spray Combustion Calculations; Int. J. Heat Mass Transf., Vol.32, p. 1605-1618, 1989

[2] R. Groll : Numerische Modellierung der Verdunstung turbulenter Zwei-Phasen-Strmungen mittels eines Euler/Euler-Verfahrens; Dissertation TU Darmstadt, Shaker Verlag Aachen, 2002

[3] R. Groll, K. Horvat, S. Jakirlić and C. Tropea: Comperative Study of Euler/Euler and Euler/Lagrange Approachs simulationg Evaporation in a Gas-Liquid Flow; 4th Int. Sym. on Turbulence, Heat and Mass Transfer, Antalya, Turkey 2003

[4] J. He und O.Simonin : Non-Equilibrium Prediction of the Particle-Phase Stress Tensor in Vertical Pneumatic Conveying; ASME, FED-Vol.166, Gas-Solid Flows, 1993

[5] J. T. Jenkins und M. W. Richman : Grad's 13-Moment-System for a Dense Gas of Inelastic Spheres; Arch. Ration. Mech. Anal., Vol.87, p. 355-177, 1985

[6] O. Kastner : Theoretische und experimentelle Untersuchungen zum Stoff''ubergang von Einzeltropfen in einem akustischen Rohrlevitator; Dissertation, Technische Fakult''at der Universit''at Erlangen-N''urnberg, 2001

[7] J. D. Kulick, J. R. Fessler und J. K. Eaton : Particle Response and Turbulence Modification in Fully Developed Channel Flow; J. Fluid Mechanics, Vol. 277, p. 109-134, Cambridge University Press, 1994

[8] P. J. Oliveira : Computer Modeling of Multidimensional Multiphase Flow and Application to T-Junctions; PhD Thesis, Empirial College London, 1992